



Optical properties of oxynitride powders

Franck Tessier, Pascal Maillard, François Cheviré, Kazunari Domen, Shinichi Kikkawa

► To cite this version:

Franck Tessier, Pascal Maillard, François Cheviré, Kazunari Domen, Shinichi Kikkawa. Optical properties of oxynitride powders. Journal of the Ceramic Society of Japan, Ceramic Society of Japan, 2009, 117 (1361), pp.1-5. <10.2109/jcersj2.117.1>. <hal-00411498>

HAL Id: hal-00411498

<https://hal.archives-ouvertes.fr/hal-00411498>

Submitted on 16 Feb 2016

HAL is a multi-disciplinary open access archive for the deposit and dissemination of scientific research documents, whether they are published or not. The documents may come from teaching and research institutions in France or abroad, or from public or private research centers.

L'archive ouverte pluridisciplinaire **HAL**, est destinée au dépôt et à la diffusion de documents scientifiques de niveau recherche, publiés ou non, émanant des établissements d'enseignement et de recherche français ou étrangers, des laboratoires publics ou privés.

Optical properties of oxynitride powders

Franck Tessier¹, Pascal Maillard¹, François Cheviré¹, Kazunari Domen², Shinichi Kikkawa³

¹ UMR CNRS 6226 "Sciences Chimiques de Rennes", équipe "Verres et Céramiques", groupe "Matériaux Nitrures", Université de Rennes 1, 35042 Rennes cedex, France

² Department of Chemical System Engineering, The University of Tokyo, 7-3-1 Hongo, Bunkyo-ku, Tokyo 113-8656, Japan

³ Graduate School of Engineering, Hokkaido University, N13W8, Kita-ku Sapporo 060-8628, Japan

* corresponding author: Franck.Tessier@univ-rennes1.fr, Fax +33 2 23 23 56 83

Keywords: Oxynitride, nitride, ceramics, optical properties, powder

Abstract

(Oxy)nitride materials have attractive properties directly related to the role played by nitrogen. A commonly used synthesis method consists of the thermal nitridation of an oxide precursor in flowing ammonia. As a consequence of the anionic N^{3-}/O^{2-} substitution results an increase in the covalent character, illustrated by a shift of the absorption edge towards higher wavelength values. Thus, oxynitrides offer potentialities as optical materials in the domain of colored pigments, UV absorbers and visible-light photocatalysts.

1. Introduction

Nitride and oxynitride materials have attractive properties directly related to the role played by nitrogen. In particular, a comparison between oxynitrides and oxides highlights the characteristics of a nitrogen N^{3-} /oxygen O^{2-} substitution: an increase in the anionic formal charge, a greater covalent character, a higher cross-linking density in glasses, a reducing character due to the N^{3-}/N^0 redox couple, and modified acid-base properties. The increase in the covalent character gives rise to interesting optical properties, for which some applications are developed below.

As observed in the UV-Vis diffuse reflectance spectra (Fig. 1), when TiO_2 is doped by nitrogen, the absorption edge is unambiguously shifted towards higher wavelengths in the visible part of the spectrum (~ 460 nm) [1].

The red shift of the absorption edge can be explained if we consider the band structure of TiO_2 , illustrated in a simplified manner in Fig. 2. The width of the forbidden band is directly related to the position of the $2p$ levels of oxygen and $3d$ levels of the transition metal. Thus, the valence band will present a predominant $2p(O)$ character while the conduction band a $3d(Ti)$ metal behavior. After doping with nitrogen, additional levels due to nitrogen confer to the valence band a $2p(N)$ behavior. The lower electronegativity of nitrogen compared to that of oxygen ($\chi_O = 3.50 > \chi_N = 3.05$) accounts for the difference in the energy level of the oxygen and nitrogen $2p$ orbitals, for example at the top of the valence band: $E_{2p}(O) = -14,8$ eV, $E_{2p}(N) = -13,4$ eV [2] and simply explains the decrease in the optical gap ($E_{gb} < 3.1$ eV $< E_{ga}$) between valence band and conduction band.

When nitriding an oxide precursor absorbing in the UV part, it is thus possible to shift the position of the absorption edge towards higher wavelengths in the visible part. Based on this specific feature of nitrogen: $\chi_N < \chi_O$, oxynitride solid solutions give the possibility to shift the position of the absorption edge by adjusting the chemical composition in both the cationic and anionic networks, which makes nitrides and oxynitrides promising as emerging materials for their optical properties. This contribution proposes to describe the results of appropriate studies recently performed in the following areas of interest: inorganic colored pigments and UV absorbers as well as visible-light driven photocatalysts.

2. Colored pigments

The color is a particularly appropriate feature to illustrate the increase in the covalent character. Whereas oxides are often colorless powders, binary nitrides display many different colors. The diversity of colors is well depicted by the following phases: Mg_3N_2 is yellow, Li_3N is red-brown and Zn_3N_2 is black. Transition metal nitrides are generally black, since the transition element does not reach its maximum oxidation state. Tantalum makes an exception, as Ta^{+V} nitride-type compounds are known: red-orange Ta_3N_5 [3-5] and yellow TaON oxynitride [6]. The color of nitride-type compounds is explained by a decrease in the band gap energy value, as confirmed by band structure calculations [7,8]. However, it is possible to maintain the highest oxidation state of transition metals in ternary oxynitrides by taking advantage of the inductive effect of an appropriate counter-cation. The corresponding compounds are found to belong to well-known structure types of the oxide crystal chemistry [9,10]. Thus, Ti^{IV} is stabilized in the perovskite $LaTiO_2N$, even though no nitrogen-richer nitride than TiN has been

prepared, and W^{VI} in the scheelite $NdWO_3N$, although the corresponding binary nitride " WN_2 " has never been isolated.

Solid solution domains are excellent candidates to link any progressive modification of the composition to that of the color. As a function of a progressive nitrogen enrichment, oxynitride solid solutions constitute a promising alternative as new colored pigments. Novel non-toxic pigments have been required to answer environmental laws to remove elements like lead, cobalt, chromium ... entering in the composition of usual pigments widely used in paintings and plastics. Jansen et al. have shown the possibility to adjust the color of oxynitride pigments in the perovskite-type system $Ca_{1-x}La_xTaO_{2-x}N_{1+x}$ [11,12]. In relation with the nitrogen content from $x = 0$ to 1, the hue varies from yellow ($CaTaO_2N$) to brown ($LaTaON_2$) through orange and deep red intermediate colors. This solid solution matches well the yellow to red colors of commercial cadmium sulphoselenide $Cd(S,Se)$ pigments, which are considered toxic.

Grins et al. have produced similar colors in the system $AZr_{1-x}Ta_xO_{3-x}N_x$ with powders evolving from the white of $AZrO_3$ to the yellow, red or brown of $ATaO_2N$, A corresponding to respectively Ca, Sr and Ba [13].

The group of Marchand prepared solid solution domains in the perovskite systems $A(A,Ta)(O,N, \ominus\ominus)_3$ ($A = Ca, Sr, Ba$) and $Sr(Sr,Nb)(O,N, \ominus\ominus)_3$ giving rise to a range of colored pigments from pale yellow to orange brown. Tests of injection in plastics have shown the stability of such phases [7]. New oxynitrides of the fluorite and perovskite-type structures have been studied for their potential as colored pigments for environmental purposes. Indeed, the progressive N^{3-}/O^{2-} anionic substitution within the

perovskite solid solution between LaTiO_2N and ATiO_3 (A=alkaline-earth) titanates results in a continuous color shift of the nitrated powders towards higher wavelength values, in agreement with a more covalent character brought by nitrogen [14]. The interest of defect fluorite rare earth tungstates - $\text{R}_6\text{WO}_{12}\square_2$ and $\text{R}_{14}\text{W}_4\text{O}_{33}\square_3$ (R = rare earth) – has been evidenced to isolate oxynitrides powders $\text{R}_6\text{W}(\text{O},\text{N},\square)_{14}$ and $\text{R}_{14}\text{W}_4(\text{O},\text{N},\square)_{36}$, the color of which changes progressively from the white of the oxides to bright yellow with increasing nitrogen substitution rate [15]. Among these oxynitride compositions, the samarium-based phase $\text{Sm}_{14}\text{W}_4\text{O}_{23.4}\text{N}_{6.4}$ is particularly attractive by its spectral characteristics and can compete with BiVO_4 , a yellow industrial pigment, as a non toxic potential challenger [10].

The behavior of the rare-earth tantalates RTaO_4 (R = La→Yb, Y) heated under ammonia at 900-950°C was recently revisited starting from precursors prepared by a ceramic route and a chimie douce process [16]. While the stoichiometry $\text{R}_2\text{Ta}_2\text{O}_5\text{N}_2$ and the pyrochlore structure were confirmed for the larger rare-earths (R = Nd→Gd), X-ray and neutron diffraction analyses have evidenced a different structure-type for the smaller rare-earths which give rise, actually, to defect fluorite solid solutions $\text{RTa}(\text{O},\text{N},\square)_4$, with R = Ho, Er, Yb and Y with variable nitrogen contents and colors. The color of $\text{YTa}(\text{O},\text{N})_4$ powders varies from yellow ($\text{YTaO}_{2.76}\text{N}_{0.83}$) to brown for the most substituted compositions ($\text{YTaO}_{2.39}\text{N}_{1.08}$). EXAFS spectra support the pyrochlore-type structure for $\text{Nd}_2\text{Ta}_2\text{O}_5\text{N}_2$ as previously presented [17]. Coordinations around both yttrium and tantalum are close to six in the $\text{YTa}(\text{O},\text{N})_4$ defect fluorite. Its crystal structure is far from an ideal fluorite but also not a simple mixture of pyrochlore antiphase domains. It is a highly defective fluorite-type structure with a random distribution of anion defects. Photoluminescence for 5 at.% doped Eu^{3+} shows the

spectra compatible with the symmetry C_{3v} lower than O_h in fluorite and D_{3d} in pyrochlore structure types for both the Gd and Y tantalum oxynitrides. These measurements support that their structure are basically pyrochlore for Nd and Gd-phases and defect fluorite for the Y one but they are highly defective. The study was then extended to the $R_2Ta-O-N$ stoichiometry. The attention was focused, in particular, on the gadolinium phase $Gd_2Ta(O,N)_4$ because of the bright yellow color of its powder [18].

Colored oxynitrides solid solution domains have also been obtained in other structure-types. Let us note, for example, orange compositions $Ta_{3-x}Zr_xN_{5-x}O_x$ ($0 \leq x \leq 0.60$) isostructural with Ta_3N_5 , and pale yellow $Ta_{1-x}Zr_xN_{1-x}O_{1+x}$ ($0 \leq x \leq 0.28$) isostructural with TaON [19].

Recently, transition metal oxynitride perovskites $A(Ta,Nb)O_2N$ ($A=Ca,Sr,Ba$) were revisited and their accurate colors were determined using a colorimeter [20]. The influence of cationic substitutions on the crystal structure was pointed up to explain the differences in colors.

From our experience, two features are important to consider a colored powder as a pigment, of course the position of the absorption edge which can be tuned at a precise value versus nitrogen content, and also its stiffness which is strongly related to the color purity.

3. UV absorbers

Most of the usual anti-UV materials are not totally satisfactory. Organic absorbers are mainly efficient in the UVB range and do not cover a large part of the UV spectra. They

are not stable and give rise sometimes to allergies. The first generation of inorganic UV absorbers is mainly based on TiO_2 and produces a whitening phenomenon due to their high refractive index. It is necessary to adapt the particule size to get a compromise between transparency and whitening. Thus, nanometric particules are required for TiO_2 , while 100 nm sized particules are enough for the competitor ZnO , characterized by a lower refractive index. A major drawback of those absorbers is their photocatalytic activity, when the surface can generate oxidizing species under irradiation, damaging the host matrix. Our group worked to finalize the preparation of a second generation of inorganic UV absorbers efficient over the whole UV part of the spectrum to incorporate them within industrial transparent finishes for wood protection purposes [21]. Among the specifications required to prepare such inorganic UV absorbers, a bandgap of exactly 3.1 eV (transition between UV and visible), a steep absorption edge and no photocatalytic activity are the most relevant. Based on the same concept of tunability of the optical absorption with the chemical composition, attempts were made to prepare solid solutions from cationic and anionic substitutions within rare earth-based oxide and oxynitride solid solutions.

We have recently reported the optical properties of fluorite-type compositions within the $\text{CeO}_2\text{-Y}_6\text{WO}_{12}$ and $\text{CeO}_2\text{-Y}_2\text{O}_3$ solid solutions and have studied their potential as inorganic UV absorber materials [22,23]. Keeping starting from the tungstate Y_6WO_{12} , we have investigated the influence of both cationic and anionic substitutions on the optical properties through the study of two fluorite-type solid solutions: $\text{Y}_6(\text{W}_{1-x}\text{Mo}_x)\text{O}_{12}$ and $\text{Y}_6\text{W}(\text{O}_{12-3/2x}\text{N}_x)$ [24]. Here, low nitrogen contents were investigated in the way to prepare white or pale yellow compositions that exhibit an absorption edge located around 400 nm (3.1 eV) giving them potential interest as inorganic UV

absorbers. The oxide precursor was prepared using the citrate route, which improves the reactivity of oxide powders with ammonia. The nitridation results in a decrease of the diffuse reflectance maximum intensity as well as in a continuous red shift of the absorption edge from 340 nm to about 525 nm. By adjusting the amount of nitrogen introduced into the yttrium tungstate structure, it becomes possible to synthesize an oxynitride composition that exhibits an absorption edge located at 400 nm, i.e. 3.1 eV (Fig. 3). However, the spectral selectivities of the nitrated compositions appear to be too low to make them suitable for any UV absorption applications.

A similar approach is presented in the case of perovskite oxide solid solutions. For example, starting from the colored perovskite oxynitride LaTiO_2N and using the following cross-substitution: $\text{La}^{\text{III}} + \text{N}^{\text{III-}} = \text{Sr}^{\text{II}} + \text{O}^{\text{II-}}$, it is possible to shift the absorption edge towards lower wavelengths [14]. We have synthesized new oxynitride solid solutions in the systems $\text{La}_{1-x}\text{A}_x\text{TiO}_{2+x}\text{N}_{1-x}$ ($\text{A} = \text{Sr}, \text{Ba}$), where it is possible to tune the color of the powders progressively from brown (LaTiO_2N), to red, orange, yellow and finally white (SrTiO_3) with the variation of both nitrogen and lanthanum contents. The green shade observed in the presence of low nitrogen contents (Fig. 4, sample b) is attributed to mixed valent titanium present in a black nitrogen-rich secondary phase: TiO_xN_y . An attenuation of this reduction phenomenon is detected when using more chemically homogeneous and reactive precursors prepared by the amorphous citrate route. Such processes bring a suitable solution to optimize the properties of (oxy)nitride materials for optical applications (colored pigments, visible-light photocatalysts...).

Avoiding such parasitic color is a major synthetic problem to solve in the preparation of light colored materials for promising applications as novel UV absorbers. Nevertheless,

the interest of oxynitride solid solution domain relies here on the possibility to tune the absorption edge position towards 400 nm, limit between the UV and the visible ranges.

4. Visible-light-driven photocatalysis

Current oxide photocatalysts (TiO_2, \dots) are wide-gap semiconductors for which UV light is necessary to produce electron-hole pairs by photoexcitation. The use of solar energy is of highest interest from a low environmental impact viewpoint. Focusing on materials absorbing in the visible part of the spectrum, nitride-type compounds, often colored, become attractive and promising for visible-light-driven photocatalysis. Two classes of materials are largely studied in literature. The first one concerns the use of nitrogen-doped oxides to decompose polluting molecules in air or water [25-28]. Among them a tremendous number of publications show the activity of nitrogen-doped titania under visible light [29-31]. The second approach is devoted to (oxy)nitrides containing more nitrogen as new materials for overall water decomposition under visible-light irradiation [32-38]. Photons with energy higher than the bandgap of the semiconductor are absorbed to form electron-hole pairs, which migrate then to the surface of the semiconducting photocatalyst (Fig. 5). The separated electrons and holes act as reducer and oxidizer, respectively in the overall water splitting reaction to produce hydrogen and oxygen.

The choice of the photocatalytic material is limited by the following specifications:

1/ the active compound should absorb the visible radiations, so the bandgap is lower than 3.1 eV but higher than the water splitting potential of 1.23 eV. 2/ efficient charge separation and fast transport of the carriers must be achieved in order to avoid

recombination between electron and hole. 3/ usually a co-catalyst (Pt, NiO, RuO₂) is loaded at the surface to increase the formation of H₂ and thus to speed the water splitting reaction. Rh_{2-x}Cr_xO₃ was tested recently as nanoparticles [35,39].

Many nitrides and oxynitrides belonging to various structure-types have been tested separately for photoreduction and photooxydation reactions using sacrificial agents, respectively with methanol (electron donor) and silver nitrate (electron acceptor). For example, TaON and CaTaO₂N manifest an activity for photoreduction and Ta₃N₅ and TaON, a strong activity for photooxydation. When ruthenium is loaded on the surface of TaON, the production of hydrogen is dramatically enhanced [40]. LaTiO₂N presents some activity for both reactions, but it decomposes slowly in water. To date only two wurtzite-type solid solutions Zn-Ga-O-N [35,36] and Zn-Ge-O-N [33,34] are efficient for overall water splitting and present a good stability as no nitrogen is released during the test. The quantum efficiencies were improved after a post treatment of the nitrated powders. A calcination of the product under nitrogen at moderate temperature allows to decrease the density of defects that act as recombination centers for photogenerated electrons and holes. Quantum efficiencies have been determined to be 5 % for Zn_{0.18}Ga_{0.82}O_{0.18}N_{0.82} and 2 % for Zn_{1.44}GeO_{0.44}N₂ under visible light. These values have to be compared with the performance of NaTaO₃ doped with lanthanum and NiO (quantum efficiency = 56%), but obtained under UV radiations (270 nm) [41]. Many experimental parameters have an influence on the results of the photocatalytic reaction. Among them, the crystallization state, the specific surface area and the zinc/germanium ratio, for example, are relevant and induce a different behavior under visible radiations, as observed for the Zn-Ge-O-N system [42].

3. Conclusion

Nitrides and oxynitrides represent a group of modern ceramic materials of increasing technological importance, with applications as hard materials, protective coatings, electronic and optical materials, refractories or structural ceramics. The incorporation of nitrogen within an oxide allows to shift the absorption edge towards visible wavelengths. Interesting optical properties are developed among pigments, UV absorption or visible-light-driven photocatalysis. The latest emerged few years ago as an original way to produce hydrogen from the overall water splitting. This approach has shown promising results which study is actually in progress.

References

- [1] C. Burda, Y. Lou, X. Chen, A. C. S. Samia, J. Stout, J. L. Gole, *Nano letters* 3, 1049-1051 (2003)
- [2] R. Hoffmann, *J. Chem. Phys.* 39, 1397-1412 (1963)
- [3] N.E. Brese, M. O’Keeffe, P. Rauch, F.J. DiSalvo, *Acta Cryst.* C47, 2291-2294 (1991).
- [4] C.M. Fang, E.Orhan, G.A. de Wijs, H.T. Hintzen, R.A. de Groot, R. Marchand, J.-Y Saillard, G. de With, *J. Mater. Chem.* 11, 1248-1252 (2001).
- [5] M. Jansen, H.P. Letschert, D. Speer, CERDEC S.A., *Eur. Pat.* n° 0 592 867 A1 (1993).
- [6] E. Orhan, F. Tessier, R. Marchand, *Solid State Sci.* 4, 1071-1076 (2002).
- [7] N. Diot, Thesis 2222, Université de Rennes 1, France (1999).
- [8] E. Orhan, S. Jobic, R. Brec, R. Marchand, J.-Y. Saillard, *J. Mater. Chem.* 12, 2475-2479 (2002).
- [9] R. Marchand, F. Tessier, A. Le Sauze, N. Diot, *Int. J. Inorg. Mater.* 3, 1143-1146 (2001).

- [10] F. Tessier, R. Marchand, *J. Solid State Chem.* 171, 143-151 (2003).
- [11] M. Jansen, H. P. Letschert, *Nature* 404, 980-982 (2000).
- [12] M. Jansen, H. P. Letschert, European patent 0627373 (1995).
- [13] J. Grins, G. Svensson, *Mater. Res. Bull.* 29, 801-809 (1994).
- [14] F. Cheviré, F. Tessier, R. Marchand, *Eur. J. Inorg. Chem.* 1223-1230 (2006)
- [15] N. Diot, O. Larcher, R. Marchand, J.Y. Kempf, P. Macaudière *J. Alloy. Compd.* 323-324, 45-48 (2001).
- [16] P. Maillard, F. Tessier, E. Orhan, F. Cheviré, R. Marchand, *Chem. Mater.* 17, 152-156 (2005).
- [17] S. Kikkawa, T. Takeda, A. Yoshiasa, P. Maillard, F. Tessier, *Mater. Res. Bull.* 43, 811-818 (2008).
- [18] P. Maillard, O. Merdrignac-Conanec, F. Tessier, *Mater. Res. Bull.* 43, 30-37 (2008).
- [19] E. Günther, M. Jansen, *Mater. Res. Bull.* 36, 1399-1405 (2001).
- [20] R. Aguiar, D. Logvinovich, A. Weidenkaff, A. Rachel, A. Reller, S.G. Ebbinghaus, *Dyes Pigments* 76, 70-75 (2008).
- [21] F. Cheviré, Thesis 3061, Université de Rennes 1, France (2004).
- [22] F. Cheviré, F. Muñoz, C.F. Baker, F. Tessier, O. Larcher, S. Boujday, C. Colbeau-Justin, R. Marchand, *J. Solid State Chem.* 179, 3184-3190 (2006).
- [23] F. Tessier, F. Cheviré, F. Muñoz, O. Merdrignac-Conanec, R. Marchand, M. Bouchard, C. Colbeau-Justin, *J. Solid State Chem.* 181, 1204-1212 (2008).
- [24] F. Cheviré, F. Clabau, O. Larcher, E. Orhan, F. Tessier, R. Marchand, *Solid State Sci.* XX, 00-00 (2008).
- [25] D. Li, H. Haneda, *J. Photochem. Photobio. A: Chem.* 155(1-3), 171-178 (2002).
- [26] D. Li, H. Haneda, *J. Photochem. Photobio. A: Chem.* 160(3), 203-212 (2003).
- [27] M. Miyauchi, M. Takashio, H. Tobimatsu, *Langmuir* 20, 232-236 (2004).
- [28] T. Murase, H. Irie, K. Hashimoto, *J. Phys. Chem. B* 108, 15803-15807 (2004).
- [29] R. Asahi, T. Morikawa, T. Ohwaki, K. Aoki, Y. Taga, *Science* 293, 269-271 (2001).

- [30] D. Li, H. Haneda, S. Hishita, N. Ohashi, *Mater. Sci. Eng. B* 117, 67-75 (2005).
- [31] E. Martinez-Ferrero, Y. Sakatani, C. Boissière, D. Grosso, A. Fuertes, J. Fraxedas, C. Sanchez, *Adv. Funct. Mater.* 17, 3348-3354 (2007).
- [32] K. Maeda, K. Domen, *J. Phys. Chem. C* 111, 7851-7861 (2007).
- [33] Y. Lee, H. Terashima, Y. Shimodaira, K. Teramura, M. Hara, H. Kobayashi, K. Domen, M. Yashima, *J. Phys. Chem. C* 111, 1042-1048 (2007).
- [34] X. Wang, K. Maeda, Y. Lee, K. Domen, *Chem. Phys. Lett.* 457, 134-136 (2008)
- [35] K. Maeda, H. Hashiguchi, H. Masuda, R. Abe, K. Domen, *J. Phys. Chem. C* 112, 3447-3452 (2008).
- [36] K. Maeda, K. Teramura, K. Domen, *J. Catal.* 254, 198-204 (2008).
- [37] D. Yamasita, T. Takata, M. Hara, J.N. Kondo, K. Domen, *Solid State Ionics* 172, 591-595 (2004).
- [38] G. Hitoki, T. Takata, J.N. Kondo, M. Hara, H. Kobayashi, K. Domen, *Electrochem.* 70, 463-465 (2002).
- [39] Y. Lee, K. Teramura, M. Hara, K. Domen, *Chem. Mater.* 19, 2120-2127 (2007).
- [40] M. Hara, J. Nunoshige, T. Takata, J.N. Kondo, K. Domen, *Chem. Commun.* 3000-3001 (2003).
- [41] A. Kudo, *Catal. Surv. Asia* 7(1), 31-38 (2003).
- [42] F. Tessier, P. Maillard, Y. Lee, K. Domen, *Mater Chem. Phys.* (2008) to be published.

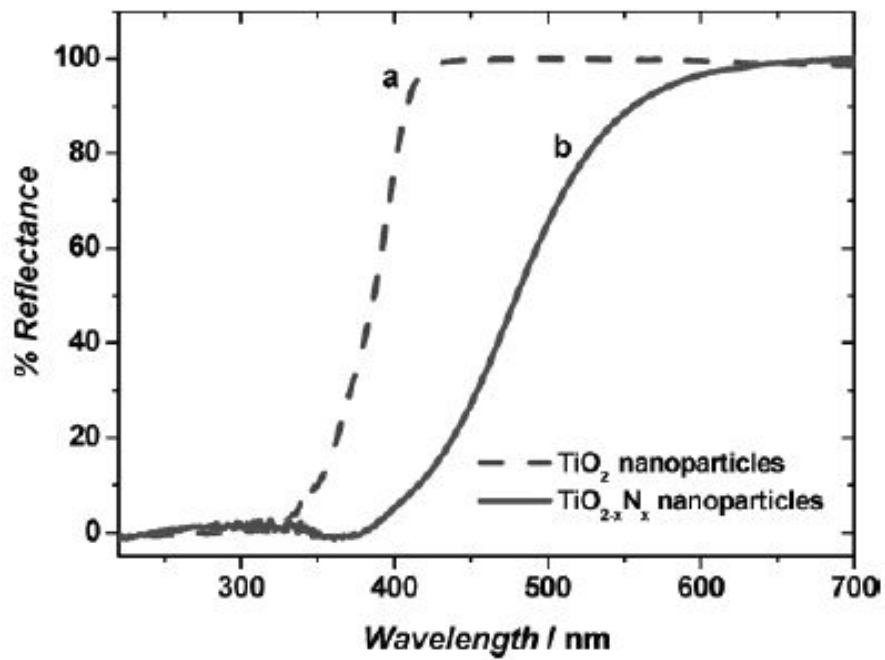


Fig. 1 : Diffuse reflectance spectra of TiO₂ and TiO_{2-x}N_x oxynitride [1].

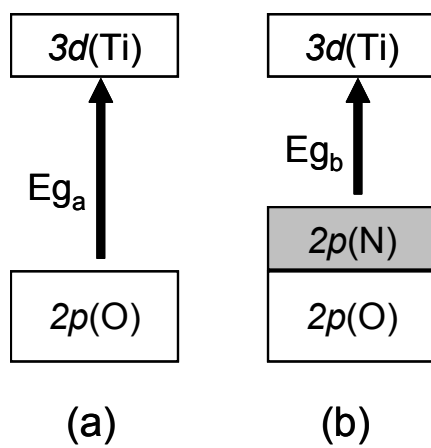


Fig. 2 : Evolution of the optical bandgap from TiO_2 (a) to nitrogen-doped $\text{TiO}_{2-x}\text{N}_x$ (b).

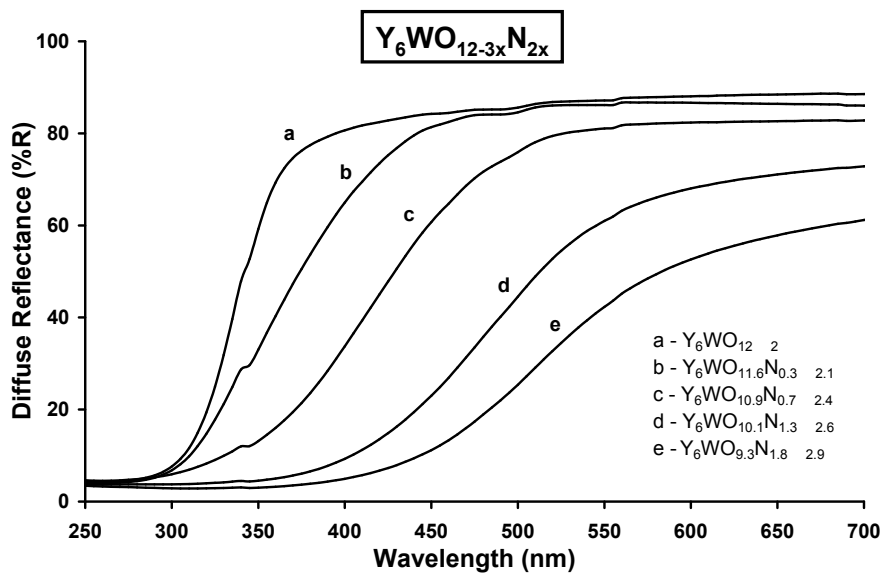


Fig. 3 : Diffuse reflectance spectra in the $Y_6WO_{12-3x}N_{2x}$ system [24].

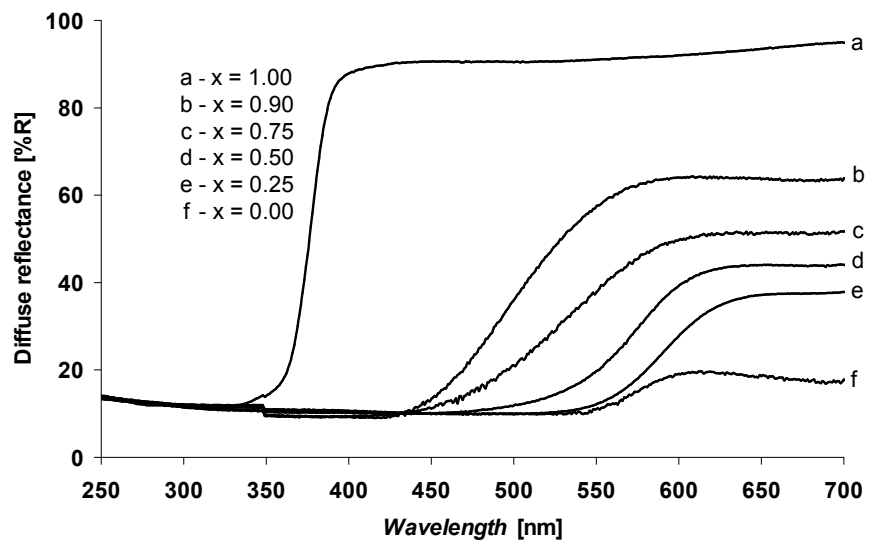


Fig. 4 : Diffuse reflectance spectra of $\text{La}_{1-x}\text{Sr}_x\text{Ti}(\text{O},\text{N})_3$ compositions [14].

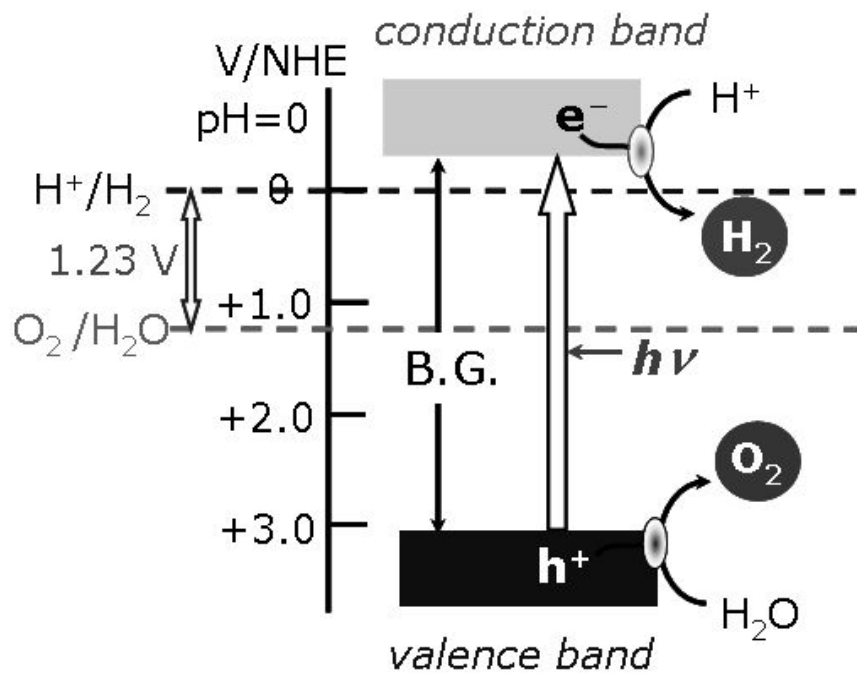


Fig. 5: Schematic of overall water splitting (from Domen et al.)